PHYSICAL REVIEW E **69**, 060701(R) (2004)

Self-assembled uniaxial and biaxial multilayer structures in chiral smectic liquid crystals frustrated between ferro- and antiferroelectricity

V. P. Panov,[1] N. M. Shtykov,[1] A. Fukuda,[1] J. K. Vij,[1,*] Y. Suzuki,[2] R. A. Lewis,[3] M. Hird,[3] and J. W. Goodby[3]
[1]*Department of Electronic and Electrical Engineering, Trinity College, University of Dublin, Dublin 2, Ireland*
[2]*Central Research Laboratory, Showa Shell Sekiyu, K. K., Kanagawa 243-0303, Japan*
[3]*Department of Chemistry, University of Hull, Hull HU6 7RX, United Kingdom*
(Received 26 September 2003; published 24 June 2004)

With a view to obtain a molecular model for the subphases produced by the frustration between ferro- and antiferroelectricity in chiral smectic liquid crystals, we report results on two compounds and observe (i) the staircase character of uniaxial SmC^*_α itself in the bulk and (ii) the multipeaked characteristic reflection bands due to the modulated helical structures just above the SmC^*_A temperature range. We suggest the emergence of several uniaxial and biaxial subphases. The results show that both types of subphases can be specified by $q_T = [F]/([A]+[F])$ in the zero-order approximation; $[A]$ and $[F]$ are the numbers of antiferroelectric and ferroelectric orderings in the unit cell. We consider the basis of both types of subphases, particularly the description of the short-pitch helical structure of SmC^*_α, in terms of the molecular models so far proposed and emphasize the important role played by the discrete flexoelectric polarization.

DOI: 10.1103/PhysRevE.69.060701 PACS number(s): 61.30.Gd, 64.70.Md, 77.80.Bh, 77.84.Nh

Ferroelectric SmC^* and antiferroelectric SmC^*_A are frustrated in chiral smectic liquid crystals. A large number of alternative structures have almost the same free energy at frustration points in the phase diagram, where the dominant synclinic and anticlinic ordering forces happen to be equal [1–4]. Long-range intermolecular interactions (LRI's), too weak to be observed ordinarily, now play a crucial role and may cause the temperature-induced successive phase transitions with staircase character. The resulting polar smectic phases, often called "subphases," consist of at least five *biaxial* subphases, characterized by periods of more than two smectic layers and providing rare examples of *ferrielectricity*, together with a *uniaxial* subphase designated as SmC^*_α [3–7]. Many sophisticated techniques have been used to determine the biaxial *nonplanar* subphase structures with three- and four-layer periodicities and the short-pitch helical structure of uniaxial SmC^*_α [8–18]. So far no unified realistic molecular model for those subphases has been reported. Two conflicting approaches have been proposed by emphasizing either the continuous short-pitch evolution of the SmC^*_α helical structure [19–22] or the staircase character of the emergence of the biaxial subphases and of SmC^*_α itself [3,4,23,24]. The first one, called the discrete clock model, takes into account competing orientational interactions between nearest- and next-nearest-neighbor smectic layers. Then the minimum of the free energy corresponds to a uniform rotation of the tilt plane about the layer normal. By introducing several other complicated interactions, we may qualitatively be able to explain the formation of subphases with three- and four-layer periodicities and the continuous evolution of short pitch in SmC^*_α. However, it is difficult to understand naturally the existence of five or more biaxial subphases.

In solid-state physics, we frequently encounter such large-scale structures as those with multilayer periodicities. The presence of some form of frustration is common to the emergence of the structures. Two statistical models have been developed that exemplify the emergence of the devil's staircase by lifting the degeneracy at the frustration points. One is the axial next-nearest-neighbor Ising (ANNNI) model used by Yamashita and Miyazima for understanding the sequence of biaxial subphases between SmC^*_A and SmC^* [4,23]. However, it is hard to visualize direct application of the Ising-like Hamiltonian to smectic liquid crystals [2]. The second model is the one-dimensional Ising model with long-range repulsion [25]. Bruinsma and Prost tried to explain the formation of SmC^*_α as well as its devil's staircase character based on this model but did not obtain the actual phase diagram [24]. They used the Casimir-type LRI due to the polarization fluctuations, which are measurable and are known to be important for dielectric behavior in SmC^*. Quite recently, Emelyanenko and Osipov [26] replaced the Ising model with a more realistic *X-Y* model and, at the same time, introduced the novel discrete flexoelectric polarization which is not parallel to the ordinary spontaneous polarization determined by the molecular chirality [26,27]. They showed that the coupling between these polarizations in adjacent layers produces an effective LRI among orientations in different layers, which stabilizes the nonplanar structures of the biaxial subphases. In particular, they predicted the existence of a number of subphases between SmC^*_A and the three-layer biaxial subphase.

Their model gives answer to the long-standing question as how to understand the existence of the biaxial and uniaxial subphases, although no detailed phase diagram has yet been obtained. This Rapid Communication provides two novel experimental observations that support the model strongly and also aims to foster further theoretical development. One is the observation of characteristic reflection bands due to the helical structures indicating the emergence of several subphases just above SmC^*_A in (*R*)-12OF1M7. The second is the result of the birefringence measurement using a photoelastic modulator (PEM) in a thick homeotropically aligned cell of

*Email address: jvij@tcd.ie

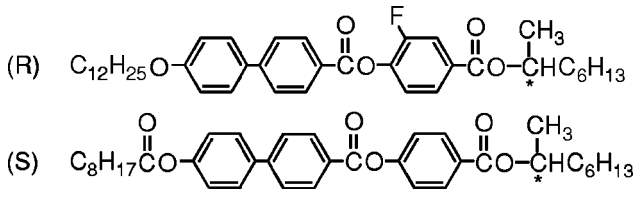

FIG. 1. Chemical formulas of the compounds used.

(*S*)-MHPOCBC and shows that uniaxial SmC^*_α consists of at least two parts. We have thus established the staircase character of both biaxial and uniaxial subphases which can reasonably be specified by $q_T=[F]/([A]+[F])$ in the zero-order approximation because of the synclinic and anticlinic frustration; $[A]$ and $[F]$ are the numbers of antiferroelectric and ferroelectric orderings in the unit cell. Hereinafter the biaxial and uniaxial subphases are designated as Sm$C^*_A(q_T)$ and Sm$C^*_\alpha(q_T)$, respectively. Figure 1 shows the chemical formulas of the samples used.

Free-standing films of 12OF1M7, 30–80 μm thick, were prepared over a hole of 2 mmϕ in a metal plate, 300 μm thick, which was mounted in an oven with temperature controlled to an accuracy of ±10 mK. The optical transmittance was measured using a spectrometer (Perkin Elmer Lambda 900). The results are summarized in Fig. 2. The full pitch band is observed in SmC^* (the left-handed helix) but not in SmC^*_A (the right-handed helix). Figure 2, inset, illustrates the half pitch band. It shows a single peak in SmC^*_A. At 79.25 °C, the band shape suddenly becomes multipeaked. There exists a temperature region 79.45–79.65 °C where exactly the same multipeaked band shapes are stably observed. Each measurement lasted 1 day after a temperature increase of 50 mK between 79.00 and 80.00 °C. Above this temperature, similar multipeaked bands were observed up to 81.50 °C by increasing the temperature in 100–200-mK steps; the averaged peak wavelength becomes monotonically longer, first

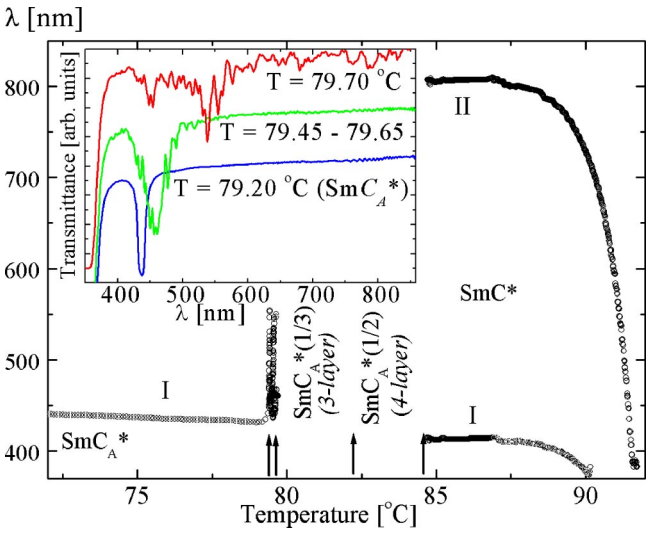

FIG. 2. (Color online) Characteristic reflection peaks for 20° oblique incidence in a 60-μm-thick free-standing film of (*R*)-12OF1M7. The inset illustrates typical characteristic reflection spectra at the indicated temperatures.

rather steeply and then gradually, up to a wavelength limit of the spectrometer, 3 μm; the stability seemed to vary from temperature to temperature. The gradual increase is consistent with the optical rotatory power (ORP) result in Sm$C^*_A(1/3)$ [18]. The characteristic reflection band could not be observed in Sm$C^*_A(1/2)$. The free-standing film, which looked uniform in SmC^*_A, now consists of several domains when the multipeaked half pitch bands are observed. The texture again becomes uniform and the half and full pitch bands are single peaked in SmC^*. The helical pitch decreases steeply in the high-temperature region and the shortest one appears to be much less than 30 smectic layers. Dielectric measurements confirm the existence of SmC^*_α above SmC^*.

Why does the half pitch band suddenly become multipeaked? The temperature variation given in Fig. 2, inset, could not be explained by the coexistence of SmC^*_A and a higher-temperature phase. The phase transition from SmC^*_A to Sm$C^*_A(1/3)$ may cause the multipeaked bands, since the helical structure of Sm$C^*_A(1/3)$ is often deformed considerably [4]. However, how can we understand the fact that the helical pitch in the stable region is very close to that of SmC^*_A? The established three-layer structure of Sm$C^*_A(1/3)$ would predict a much longer helical pitch even if the large distortion from the planar structure were taken into account. Moreover, why does the stable region exist? On considering the synclinic and anticlinic frustration, it is natural to conclude that these half pitch bands primarily correspond to the subphases predicted by Emelyanenko and Osipov and specified by q_T's [26]. In a crude approximation, the helical pitch $p(q_T)$ of a subphase specified by q_T is given by $1/p(q_T)=(1-q_T)/p_{CA}+q_T/p_C$. On using $p_{CA}=434$ nm and $p_C=-409$ nm, we obtain $p(1/9)=563$ nm and $p(1/19)=490$ nm. Furthermore, surface effects together with variations in the number of smectic layers from place to place in the free-standing film complicate the half pitch bands. If the total number of layers is not a multiple of the period of a subphase, the remaining layers may give rise to strong surface effects [26]. Since the difference in the free energy between subphases with small q_T's (large periods) becomes extremely small, such surface effects easily modulate the ideal helical structure of Sm$C^*_A(q_T)$ and produce several side peaks and the observed multidomain texture. Even the intrinsic instability as discussed in Sm$C^*_A(1/3)$ [4] may also cause additional modulation.

Figure 3 shows the birefringence as a function of the electric field and temperature observed in a homeotropically aligned cell of 25 μm thickness. The electric field was applied by using indium-tin-oxide (ITO) electrodes separated by 55 μm. Since the laser beam spot is slightly larger than the gap and the field within the area of the beam spot cannot be uniform, the absolute value may differ from the true value somewhat. The SmC^*_α temperature range was also confirmed independently by dielectric measurements using a homogeneous cell. Figure 3 clearly shows that SmC^*_α is quite uniaxial with negligible ORP at $E=0$ and, more importantly, SmC^*_α consists of at least two parts. Takanishi *et al.* and Hiraoka *et al.* (references to their work given in the review article by Fukuda *et al.* [3]) had observed in preliminary switching current investigations that SmC^*_α is not a simple

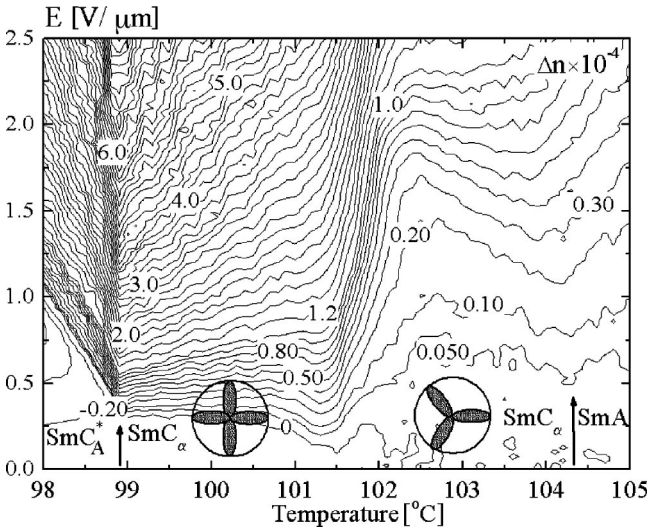

FIG. 3. *E-T* phase diagram of the field-induced birefringence in a 25-μm-thick homeotropic cell of (*S*)-MHPOCBC. The labels of constant birefringence correspond to values $\Delta n \times 10^{-4}$.

single phase and had concluded that the high- and low-temperature parts look like antiferroelectric and ferrielectric, respectively. Since they used rather thin homogeneous cells, their conclusions were not free from a possibility that the surface effects might have partly accounted for these observations. Quite recently, Cady *et al.* [28] also studied the short-pitch helical structure of MHPOCBC by using much thinner free-standing films with 50–100 smectic layers and concluded that the pitch continuously becomes shorter with decreasing temperature. However, they did not clarify the existence of the two parts in SmC^*_α. Probably, their results are influenced considerably by the surface effects. From Figs. 2 and 3, the staircase character of the biaxial subphases and uniaxial SmC^*_α itself is firmly established in the bulk; hence we consider the description of Sm$C^*_\alpha(q_T)$ and Sm$C^*_A(q_T)$ in terms of the molecular models so far proposed.

The fundamental phases—ferroelectric SmC^* and antiferroelectric SmC^*_A—are stabilized by short-range intermolecular interactions (SRI's), which were studied in detail by Osipov and Fukuda [2]. The tilting is mainly caused by the intralayer SRI's and the corresponding free energy is written in terms of the Landau expansion as

$$\tilde{F}_\perp(\Theta) = \alpha(\tilde{T} - 1)\sin^2\Theta + B\sin^4\Theta. \tag{1}$$

Here Θ is the tilt angle, $\tilde{T} = T/T^*$ is dimensionless temperature normalized by T^* (the phase transition temperature between Sm*A* and SmC^* or SmC^*_A), and $\alpha > 0$ and $B > 0$ are ordinary temperature-independent dimensionless constants. The normalized free energy difference between SmC^* and SmC^*_A, $\tilde{F}_C - \tilde{F}_{CA}$, mainly results from the interlayer SRI's and is written as

$$\Delta\tilde{F}_\parallel(\Theta) = \sin^2 2\Theta\left(-\tilde{V}_\parallel + \frac{\tilde{d}_\perp^4}{\tilde{T}\cos^6\Theta}\right). \tag{2}$$

Here $\tilde{V}_\parallel$ is a dimensionless coefficient stabilizing SmC^*, which originates from the packing entropy, the Maier-Saupe-type dispersion force, etc., and $\tilde{d}_\perp$ is a dimensionless transverse dipole moment. It should be noted that the orientational correlation (dynamic pairing) of the transverse dipole moments in adjacent layers plays an important role in stabilizing SmC^*_A [2,3]. Figure 4 illustrates the phase diagram and the temperature variation of the free energy difference thus obtained, which are characterized by only two parameters α/B and $\tilde{d}_\perp^4/\tilde{V}_\parallel$. Here α/B describes the temperature variation of Θ in Eq. (1). The synclinic ferroelectric and anticlinic antiferroelectric phases thus produced are frustrated because of the low-energy barrier between them together with the *X*-*Y* freedom [2,27]. When $\tilde{d}_\perp^4/\tilde{V}_\parallel < 1$, in particular, there exist two frustration points P_A and P_α, which produce Sm$C^*_A(q_T)$ and Sm$C^*_\alpha(q_T)$, respectively. In the zero-order approximation, the subphase has a planar structure specified by q_T and its free energy is given by

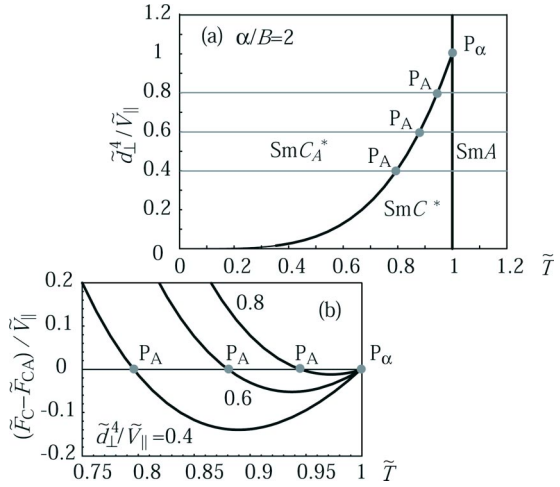

FIG. 4. Phase diagram for $\alpha/B = 2$ and free energy difference between SmC^* and SmC^*_A for $\tilde{d}_\perp^4/\tilde{v}_{eff}^\parallel = 0.4$, 0.6, and 0.8.

$$\tilde{F}(q_T) = q_T\tilde{F}_C + (1 - q_T)\tilde{F}_{CA}. \tag{3}$$

Without considering any LRI's, none of the subphases has a free energy lower than that of the fundamental phase stable at a particular temperature, SmC^*_A or SmC^*, and the degeneracy at the frustration points is not lifted.

Degeneracy lifting at the frustration points has not been analyzed fully by taking account of the temperature variation of Θ. The effective LRI was studied by assuming $\Theta = \text{const}$ [26]. The temperature variation of Θ was taken into account in the investigation of the Casimir-type LRI [27], but both the ordinary polarization due to the molecular chirality and the discrete flexoelectric polarization, which are not parallel to each other, could not be treated appropriately by the equation reported by Bruinsma and Prost [24]. Provided that the free energy difference and the LRI's are calculated appropriately, a variety of experimentally observed subphase sequences can be explained by the degeneracy lifting in Fig 4. Isozaki *et al.* studied five binary mixture systems experimentally and concluded that it is useful to consider the strength of antiferroelectricity and that of ferroelectricity work summarized in review articles [3,4]. The ordinate in Fig. 4,

$\tilde{d}_{\perp}^{4}/\tilde{V}_{\parallel}$, actually measures the relative strength. No subphases emerge for $\tilde{d}_{\perp}^{4}/\tilde{V}_{\parallel} > 1$. When $\tilde{d}_{\perp}^{4}/\tilde{V}_{\parallel} \approx 1$, Sm$C_{\alpha}^{*}$ alone appears. As the parameter becomes smaller, first Sm$C_{A}^{*}(1/3)$, then Sm$C_{A}^{*}(1/2)$, and finally SmC^{*} emerge; all of these three coexist for a while. By further decreasing this parameter, first Sm$C_{A}^{*}(1/2)$ and then SmC_{α}^{*} disappears; Sm$C_{A}^{*}(1/3)$ seems to be the most stable subphase when $\tilde{d}_{\perp}^{4}/\tilde{V}_{\parallel} < 1$. Regarding subphases in the regions of $q_T < 1/3$, $1/3 < q_T < 1/2$, and $1/2 < q_T$, at least one stable subphase is confirmed to exist in each region [3–7]. The $q_T < 1/3$ region exists in the widest parameter range of $\tilde{d}_{\perp}^{4}/\tilde{V}_{\parallel}$ and hence is most easily observable; in particular, several subphases are stabilized in 12OF1M7 here investigated. On the other hand, the observable parameter range for the $q_T > 1/2$ region seems to be the narrowest.

The phase diagram shown in Fig. 4 is also useful for understanding the staircase character of SmC_{α}^{*} itself. In the case of the biaxial subphases, Sm$C_{A}^{*}(1/3)$ and Sm$C_{A}^{*}(1/2)$ are relatively stable. It is natural to consider that three-layer Sm$C_{\alpha}^{*}(1/3)$ and four-layer Sm$C_{\alpha}^{*}(1/2)$ are also relatively stable. Since the temperature dependence of the free energy difference has just opposite gradient at the two frustration points, Sm$C_{\alpha}^{*}(1/2)$ must emerge on the low-temperature side of Sm$C_{\alpha}^{*}(1/3)$. At the same time, very large nonplanar distortions must be caused by the LRI's, since the free energy barrier is proportional to $\sin^2 2\Theta$ [27] and the tilt angle is less than 5°in SmC_{α}^{*}. Consequently, Sm$C_{\alpha}^{*}(1/2)$ and Sm$C_{\alpha}^{*}(1/3)$ are found to be quite uniaxial. The competing orientational interactions in the discrete clock model may also play an important role and cause a steep decrease in the helical pitch as a pretransitional effect in SmC^{*}. The steric interactions within a single layer and between adjacent layers were considered as a molecular manifestation of such competing orientational interactions. Because of their highly symmetric uniaxial structure, the spontaneous polarizations are canceled out within the unit cells; hence both of them are antiferroelectric like. By considering the switching behavior in Sm$C_{A}^{*}(1/2)$ and Sm$C_{A}^{*}(1/3)$, switching occurs from Sm$C_{\alpha}^{*}(1/2)$ into SmC^{*} indirectly via Sm$C_{\alpha}^{*}(1/3)$ while directly from Sm$C_{\alpha}^{*}(1/3)$ to SmC^{*}; this is in accordance with the previous observations by Takanishi *et al.* and reviewed by Fukuda *et al.* [3]. The ordinary rather weak chiral interaction may lead to a choice between the left-handed or the right-handed structure and this apparently produces the short-pitch helical structure.

We thank the SFI and EU (SAMPA project) for funding of the research work.

[1] E. Gorecka, D. Pociecha, M. Glogarova, and J. Mieczkowski, Phys. Rev. Lett. **81**, 2946 (1998).
[2] M. A. Osipov and A. Fukuda, Phys. Rev. E **62**, 3724 (2000).
[3] A. Fukuda, Y. Takanishi, T. Isozaki, K. Ishikawa, and H. Takezoe, J. Mater. Chem. **4**, 997 (1994) and references therein.
[4] T. Matsumoto, A. Fukuda, M. Johno, Y. Motoyama, T. Yui, S. S. Seomun, and M. Yamashita, J. Mater. Chem. **9**, 2051 (1999) and references therein.
[5] T. Isozaki, T. Fujikawa, H. Takezoe, T. Hagiwara, Y. Suzuki, and I. Kawamura, Jpn. J. Appl. Phys., Part 2 **31**, L1435 (1992).
[6] J. Hatano, Y. Hanakai, H. Furue, H. Uehara, S. Saito, and K. Murashiro, Jpn. J. Appl. Phys., Part 1 **33**, 5498 (1994).
[7] Yu. P. Panarin, O. Kalinovskaya, J. K. Vij, and J. W. Goodby, Phys. Rev. E **55**, 4345 (1997).
[8] P. Mach, R. Pindak, A.-M. Levelut, P. Barois, H. T. Nguyen, C. C. Huang, and L. Furenlid, Phys. Rev. Lett. **81**, 1015 (1998).
[9] A.-M. Levelut and B. Pansu, Phys. Rev. E **60**, 6803 (1999).
[10] V. Laux, N. Isaert, G. Joly, and H. T. Nguyen, Liq. Cryst. **26**, 361 (1999).
[11] T. Akizuki, K. Miyachi, Y. Takanishi, K. Ishikawa, H. Takezoe, and A. Fukuda, Jpn. J. Appl. Phys., Part 1 **38**, 4832 (1999).
[12] P. M. Johnson, S. Pankratz, P. Mach, H. T. Nguyen, and C. C. Huang, Phys. Rev. Lett. **83**, 4073 (1999).
[13] P. M. Johnson, D. A. Olson, S. Pankratz, H. Nguyen, J. Goodby, M. Hird, and C. C. Huang, Phys. Rev. Lett. **84**, 4870 (2000).
[14] L. S. Matkin, S. J. Watson, H. F. Gleeson, R. Pindak, J. Pitney, P. M. Johnson, C. C. Huang, P. Barois, A.-M. Levelut, G. Srajer, J. Pollmann, J. W. Goodby, and M. Hird, Phys. Rev. E **64**, 021705 (2001).
[15] N. M. Shtykov, J. K. Vij, R. A. Lewis, M. Hird, and J. W. Goodby, Liq. Cryst. **28**, 1699 (2001).
[16] H. Orihara, A. Fajar, and V. Bourny, Phys. Rev. E **65**, 040701(R) (2002).
[17] A. Fajar, H. Murai, and H. Orihara, Phys. Rev. E **65**, 041704 (2002).
[18] V. P. Panov, J. K. Vij, N. M. Shtykov, S. S. Seomun, D. D. Parghi, M. Hird, and J. W. Goodby, Phys. Rev. E **68**, 021702 (2003).
[19] H. Sun, H. Orihara, and Y. Ishibashi, J. Phys. Soc. Jpn. **62**, 2706 (1993).
[20] A. Roy and N. V. Madhusudana, Europhys. Lett. **41**, 501 (1998).
[21] M. Cepic and B. Zeks, Phys. Rev. Lett. **87**, 085501 (2001).
[22] D. A. Olson, X. F. Han, A. Cady, and C. C. Huang, Phys. Rev. E **66**, 021702 (2002).
[23] M. Yamashita and S. Miyazima, Ferroelectrics **148**, 1 (1993).
[24] R. Bruinsma and J. Prost, J. Phys. II **4**, 1209 (1994).
[25] R. Bruinsma and P. Bak, Phys. Rev. B **27**, 5824 (1983).
[26] A. V. Emelyanenko and M. A. Osipov, Phys. Rev. E **68**, 051703 (2003).
[27] A. Fukuda, H. Hakoi, M. Sato, and M. A. Osipov, Mol. Cryst. Liq. Cryst. Sci. Technol., Sect. A **398**, 169 (2003).
[28] A. Cady, X. F. Han, D. A. Olson, H. Orihara, and C. C. Haung, Phys. Rev. Lett. **91**, 125502 (2003).